

Constraints on Parameter Space from Perturbative Unitarity in Models with Three Scalar Doublets

Stefano Moretti^{1,*} and Kei Yagyu^{1,†}

¹*School of Physics and Astronomy, University of Southampton,
Southampton, SO17 1BJ, United Kingdom*

Abstract

We calculate an s -wave amplitude matrix for all the possible 2-to-2 body scalar boson elastic scatterings in models with three scalar doublets, including contributions from the longitudinal component of weak gauge bosons via the Equivalence Theorem Approximation. Specifically, we concentrate on the two cases with two[one] active plus one[two] inert doublet fields, referred to as I(1+2)HDM[I(2+1)HDM], under CP conservation. We obtain three analytically irreducible sub-matrices with the 3×3 form and eighteen eigenvalues for the amplitude matrix as an independent set, where the same formula can be applied to both models. By requiring a perturbative unitarity condition, we can constrain the magnitude of quartic coupling constants in the Higgs potential. This constraint, in particular in the I(1+2)HDM, can be translated into a bound on masses of extra active scalar bosons. Furthermore, when Standard Model-like Higgs boson couplings with weak gauge bosons are deviated from the Standard Model predictions, the unitarity condition provides an upper limit on the masses. We find that stronger upper bounds on the masses of the active CP-even and CP-odd Higgs bosons are obtained under the constraints from the unitarity and vacuum stability conditions, as well as the electroweak S , T and U parameters, as compared to those in 2-Higgs Doublet Models with a softly-broken Z_2 symmetry.

PACS numbers:

*Electronic address: S.Moretti@soton.ac.uk

†Electronic address: K.Yagyu@soton.ac.uk

I. INTRODUCTION

After the completion of the operations for LHC Run-I, the most important legacy for the whole of particle physics is the existence of a Higgs boson with a mass of about 126 GeV [1]. Furthermore, as a result of combined data from various Higgs search channels, it was established that the observed Higgs boson has properties which are consistent with those of the Standard Model (SM) Higgs state [2].

However, it is natural to be left with a key question. Namely, what is the actual number of scalar doublet fields present in Nature? Although the Higgs sector in the SM is constructed of only one isospin doublet field, that is not supported by a fundamental principle. In fact, it is well known that multi-doublet models can be considered so that the Higgs boson phenomenology is consistent with current LHC data by arranging additional parameters suitably, and they are often introduced new physics models beyond the SM.

For example, Supersymmetry-extended models require at least two doublets in their Higgs sector for gauge anomaly cancellation and to construct the Yukawa Lagrangian [3]. A second doublet field is introduced also in many radiative neutrino mass models [4]. The Inert Doublet Model (IDM) [5], aka a 2-Higgs Doublet Model (2HDM) with one active and one inert doublet, has been proposed to explain the existence of Dark Matter (DM), by depriving a Vacuum Expectation Value (VEV) of the second doublet field and making it non-interacting with SM fields except for the (thereby active) Higgs boson itself and the gauge states¹. Furthermore, an additional source of CP-violation is obtained in a Higgs sector with multiple doublets which is required to realize a successful scenario for Electro-Weak (EW) baryogenesis [6].

Properties of an enlarged Higgs sector clearly depend on the new physics scenario embedding it, so that the determination of the true Higgs boson dynamics is extremely important to extract information on the new physics model. In particular, if a multi-doublet structure is chosen for the Higgs sector, what is a mass scale of the additional active and/or inert (pseudo)scalar bosons? How can we extract information on the total number of doublet fields? Needless to say, the direct way to probe a multi-doublet structure is discovering extra (pseudo)scalar bosons at collider experiments. For example, even in the simplest case of 2HDMs, there appear a pair of singly-charged (H^\pm), a CP-odd (A) and a CP-even (H) Higgs boson in addition to the SM-like Higgs boson (h). Clearly,

¹ This can be simply realized by imposing an additional unbroken discrete Z_2 symmetry into the Higgs sector, where all the SM particles [the second doublet] are assigned to be even [odd] under the Z_2 symmetry. The particles with the odd parity are produced in pairs and the lightest one amongst these is stable, hence a DM candidate.

the most important property to find these extra scalar bosons is their masses.

Although, in general, these masses are taken as free parameters, we may be able to constrain their corresponding parameter space by taking into account theoretical constraints: chiefly, perturbative unitarity and vacuum stability. In 2HDMs, the unitarity and vacuum stability bounds have been discussed in Refs. [7, 8] and in Ref. [9], respectively. By using them, dimensionless parameters in the scalar potential can be constrained, and it can be translated into limits on the mass parameters for the extra (pseudo)scalar bosons. In particular, when there is a non-zero mixing between h and H in 2HDMs, the exact decoupling limit of the extra scalar boson can no longer be taken, because of the unitarity constraints. Therefore, one can obtain an upper limit on the mass of the extra scalar boson [10]. The argument can be generalized to multi-Higgs doublet scenarios.

The effects of a non-zero mixing can appear as deviations in the couplings of h with gauge bosons (hVV) and/or fermions ($hf\bar{f}$) from the SM predictions. Hence, the very fact that the latter can be accessed experimentally enables one to extract information on the underlying (pseudo)scalar dynamics above and beyond the mass scale directly probed at the collider concerned. Take the hVV couplings for example. They are presently (i.e., after LHC Run-I) constrained to be SM-like at the level of 10% or so. LHC Run-II (13 TeV) at standard integrated luminosity (300 fb^{-1}) would improve this precision by about a factor of 2. Their expected accuracy will then be about 2% [11] at the High-Luminosity (HL) LHC [12] (with collision energy of 14 TeV and integrated luminosity of 3000 fb^{-1}). Furthermore, the accuracy is expected to be about 0.4% [11] at the International Linear Collider (ILC) with collision energy of 500 GeV and integrated luminosity of 500 fb^{-1} (ILC500). Therefore, if a deviation in hVV couplings is discovered at future colliders, whenever this will occur, it will at the same time suggest the possibility of an enlarged Higgs sector and, if so, enable one to place an upper limit on the mass of extra (pseudo)scalar bosons.

In this paper, we investigate constraints on dimensionless parameters in the scalar potential from the bounds imposed by perturbative unitarity and vacuum stability in 3-Higgs Doublet Models (3HDMs). The phenomenological importance of such extended Higgs scenarios, amongst many possible others, has been emphasized lately in the context of the latest LHC results and DM searches. For example, 3HDMs may shed light on the flavour problem, namely the unknown origin and nature of the three families of quarks and leptons, including neutrinos, and their pattern of masses, mixings and CP violation: it is possible that the three families of quarks and leptons could be described by the same symmetries that describe the three Higgs doublets [13, 14]. Such a family symmetry could be spontaneously broken along with the EW symmetry, although some remnant subgroup could survive, thereby stabilizing a possible scalar DM candidate while for

certain symmetries it is possible to find a VEV alignment that respects the original symmetry of the potential which will then be responsible for the stabilization of the DM candidate [15].

Although there are several types of 3HDMs depending on symmetries imposed in the scalar potential [16]–[20], having in view the aforementioned phenomenological requirements and a need for a simple and predictive formulation, recently, Z_2 symmetric 3HDMs with one or two inert doublets have been investigated and found viable from both a DM and LHC perspective [21, 22]. Furthermore, other than explaining current data, new regions of DM relic density and areas of parameter space yielding totally new LHC signals (with respect to, e.g., 2HDMs) open up [21–23].

Herein, we focus on the I(1+2)HDM and I(2+1)HDM, where the former[latter] model contains two[one] active doublets and one[two] inert doublets. We calculate the s -wave amplitude matrix for all possible 2-to-2 body scalar boson elastic scatterings in the high energy limit in both models, including contributions from the SM gauge bosons as the Nambu-Goldstone (NG) boson states due to the Equivalence Theorem Approximation (ETA)². We then examine the allowed parameter space from the unitarity and vacuum stability (re-derived herein and found to be compliant with those in Refs. [21]) bounds in addition to the constraints from the S , T and U parameters. Then, as intimated, we proceed to apply the unitarity bounds to obtain an upper limit on the masses of A and H in the I(1+2)HDM in the case with a non-zero mixing between h and H , and study how the limit can be changed as compared to that in 2HDMs. We find that a stronger upper bound is obtained in the I(1+2)HDM than that in 2HDMs depending on the masses of the inert (pseudo)scalar bosons. Therefore, we can exclude the I(1+2)HDM when the masses of A or H will be found to be larger than the given upper limit for a fixed amount of the mixing between h and H . As for the I(2+1)HDM, since unitarity here is perfectly realized by the SM-like Higgs state h , we study what constraints are induced on the various parameters in the potential involving inert states) in order not to spoil the perturbative behavior of the only active scalar in this scenario.

This paper is organized as follows. In Sec. II, we give the scalar potential and mass formulae for the scalar bosons. In Sec. III, constraints from vacuum stability, perturbative unitarity and the S , T and U parameters are discussed. In Sec. IV, we delineate the allowed parameter regions from the constraints given in the preceding section. Finally, conclusions are given in Sec. V.

² In Ref. [20], the similar approach has been applied to a 3HDM with a non-Abelian discrete S_3 symmetry to obtain eigenvalues for the s wave amplitude matrix. Because the symmetry imposed in the Higgs potential in our paper is different from that in Ref. [20], derived eigenvalues are also different. We have confirmed that our formula for the eigenvalues coincides with those presented in Ref. [20] by taking appropriate replacements of the coupling constant in the potential. Detailed explanations are given in the end of Sec. III-B.

	I(1+2)HDM			I(2+1)HDM		
Doublet	φ_0	φ_1	φ_2	φ_0	φ_1	φ_2
Z_2	-	+	+	+	-	-
\tilde{Z}_2	+	+	-	+	+	-

TABLE I: Charge assignment under the $Z_2 \times \tilde{Z}_2$ symmetry in the I(1+2)HDM and I(2+1)HDM.

II. THREE HIGGS DOUBLET MODELS

A. The scalar potential

Among various classes of 3HDMs [17], we discuss the one which satisfies the following requirements:

- (i) it contains a SM-like Higgs boson;
- (ii) it contains a unique candidate of DM in a given mass spectrum;
- (iii) it does not have Flavour-Changing Neutral Current (FCNCs) at the tree level.

In order to satisfy the requirements of (i) and (ii), we need at least one active and one inert doublet field. Thus, the (pseudo)scalar sector of our 3HDMs must be composed of one inert plus two active doublet fields; i.e., I(1+2)HDM or two inert plus one active doublet fields; i.e., I(2+1)HDM. To guarantee a doublet field being inert and the stability of a DM candidate, we require the corresponding VEV to be zero and impose an unbroken discrete Z_2 symmetry onto the whole doublet sector. A DM candidate can then be obtained as the lightest neutral (pseudo)scalar component of the inert doublet field with the odd parity under Z_2 (the SM plus the Higgs/active (pseudo)scalar states being even). As a consequence, we also obtain that the inert (pseudo)scalar states can only appear in pairs in each vertex in the Lagrangian, so that they cannot couple to fermions directly. In the I(1+2)HDM, FCNC processes via neutral scalar boson mediation appear at the tree level similarly to the generic 2HDM case, because of the existence of two doublet fields with the same quantum numbers. The simplest way to avoid such FCNCs is imposing another discrete Z_2 symmetry [24] which can be softly-broken in general (henceforth denoted as \tilde{Z}_2). Here, we consider both the I(1+2)HDM and I(2+1)HDM with the two discrete symmetries Z_2 and \tilde{Z}_2 ³.

³ In the I(2+1)HDM, there is no FCNC at the tree level even when we do not impose the \tilde{Z}_2 symmetry. However, by imposing the \tilde{Z}_2 symmetry throughout, the structure of the Higgs potential can be much simpler than that

To write down the scalar potential in the 3HDMs, let φ_i ($i = 0, \dots, 2$) be isospin doublet scalar fields, where the assignment of $Z_2 \times \tilde{Z}_2$ charge is listed in Table I. The most general scalar potential is then given in the same form in both the I(1+2)HDM and I(2+1)HDM by

$$\begin{aligned}
V(\varphi_0, \varphi_1, \varphi_2) = & \sum_{i=0, \dots, 2} \mu_i^2 \varphi_i^\dagger \varphi_i + (\mu_{12}^2 \varphi_1^\dagger \varphi_2 + \text{h.c.}) \\
& + \frac{1}{2} \sum_{i=0, \dots, 2} \lambda_i (\varphi_i^\dagger \varphi_i)^2 + \lambda_3 (\varphi_1^\dagger \varphi_1) (\varphi_2^\dagger \varphi_2) + \lambda_4 |\varphi_1^\dagger \varphi_2|^2 + \frac{1}{2} [\lambda_5 (\varphi_1^\dagger \varphi_2)^2 + \text{h.c.}] \\
& + \rho_1 (\varphi_1^\dagger \varphi_1) (\varphi_0^\dagger \varphi_0) + \rho_2 |\varphi_1^\dagger \varphi_0|^2 + \frac{1}{2} [\rho_3 (\varphi_1^\dagger \varphi_0)^2 + \text{h.c.}] \\
& + \sigma_1 (\varphi_2^\dagger \varphi_2) (\varphi_0^\dagger \varphi_0) + \sigma_2 |\varphi_2^\dagger \varphi_0|^2 + \frac{1}{2} [\sigma_3 (\varphi_2^\dagger \varphi_0)^2 + \text{h.c.}], \tag{1}
\end{aligned}$$

where μ_{12}^2 , λ_5 , ρ_3 and σ_3 are complex parameters in general. Throughout the paper, we take these parameters to be real for simplicity, thereby avoiding explicit CP violation. We also neglect the possibility of complex VEVs, thus also removing spontaneous CP violation. Hence, the (pseudo)scalar fields can be parameterised as

$$\varphi_i = \begin{bmatrix} H_i^+ \\ \frac{1}{\sqrt{2}}(H_i + v_i + iA_i) \end{bmatrix}, \quad (i = 0, \dots, 2), \tag{2}$$

where v_i are the VEVs of φ_i with the sum rule $\sum_i v_i^2 = v^2 \simeq (246 \text{ GeV})^2$. In the I(2+1)HDM, $v_1 = v_2 = 0$ and $v_0 = v$ while in the I(1+2)HDM, $v_1, v_2 \neq 0$ and $v_0 = 0$.

The Yukawa Lagrangian in the I(2+1)HDM is given in the same form as that in the SM, where φ_0 gives all the SM fermion masses. In contrast, in the I(1+2)HDM, the structure of the Yukawa Lagrangian depends on the \tilde{Z}_2 charge assignments for the SM fermions. In general, there are four independent choices of the assignment [25, 26] and these are the so-called Type-I, Type-II, Type-X and Type-Y [27]. Various constraints from flavour [28] and collider physics [10, 27, 29, 30] strongly depend on this choice. However, the following discussion does not, though we will make sure to avoid phenomenologically dangerous regions of parameter space.

B. Mass formulae in the I(1+2)HDM

In the I(1+2)HDM, the inert sector is composed of one doublet. Therefore, the CP-even, CP-odd and pair of charged scalar states in the doublet field φ_0 correspond to the mass eigenstates.

in the case without it, thereby rendering possible a semi-analytical treatment of unitarity violating processes. In this connection, it turns out that we can deal with the two models uniformly as seen in the scalar potential (given below in Eq. (1)). We thus consider the $Z_2 \times \tilde{Z}_2$ symmetric potential in both 3HDMs.

To avoid a confusion between the inert and active scalar states, we represent the inert states H_0^\pm , A_0 and H_0 as η^\pm , η_A and η_H , respectively. Their masses are calculated as

$$m_{\eta^\pm}^2 = \mu_0^2 + \frac{v^2}{2} [\rho_1 \cos^2 \beta + \sigma_1 \sin^2 \beta], \quad (3)$$

$$m_{\eta_H}^2 = \mu_0^2 + \frac{v^2}{2} [(\rho_1 + \rho_2 + \rho_3) \cos^2 \beta + (\sigma_1 + \sigma_2 + \sigma_3) \sin^2 \beta], \quad (4)$$

$$m_{\eta_A}^2 = \mu_0^2 + \frac{v^2}{2} [(\rho_1 + \rho_2 - \rho_3) \cos^2 \beta + (\sigma_1 + \sigma_2 - \sigma_3) \sin^2 \beta]. \quad (5)$$

The mass formulae for the active sector are completely the same as those in a generic 2HDM, so that we can directly apply the same mass formulae to the I(1+2)HDM. The mass eigenstates for the active scalar bosons are thus given as:

$$\begin{pmatrix} H_1^\pm \\ H_2^\pm \end{pmatrix} = R(\beta) \begin{pmatrix} G^\pm \\ H^\pm \end{pmatrix}, \quad \begin{pmatrix} A_1 \\ A_2 \end{pmatrix} = R(\beta) \begin{pmatrix} G^0 \\ A \end{pmatrix}, \quad \begin{pmatrix} H_1 \\ H_2 \end{pmatrix} = R(\alpha) \begin{pmatrix} H \\ h \end{pmatrix},$$

with $R(\theta) = \begin{pmatrix} \cos \theta & -\sin \theta \\ \sin \theta & \cos \theta \end{pmatrix}$, (6)

where G^\pm and G^0 are the NG bosons which are absorbed by a longitudinal component of the W^\pm and Z bosons, respectively, and h is the SM-like Higgs boson. The mixing angle β is expressed by the ratio of the VEVs as $\tan \beta = v_2/v_1$.

The squared masses of H^\pm and A are then calculated as

$$m_{H^\pm}^2 = M^2 - \frac{v^2}{2}(\lambda_4 + \lambda_5), \quad m_A^2 = M^2 - v^2 \lambda_5, \quad (7)$$

where

$$M^2 = -\frac{\mu_{12}^2}{\sin \beta \cos \beta}. \quad (8)$$

The mass matrix for the neutral CP-even (scalar) states is expressed in terms of β and the usual mixing angle α as

$$m_H^2 = \cos^2(\alpha - \beta)M_{11}^2 + \sin^2(\alpha - \beta)M_{22}^2 + \sin 2(\alpha - \beta)M_{12}^2, \quad (9)$$

$$m_h^2 = \sin^2(\alpha - \beta)M_{11}^2 + \cos^2(\alpha - \beta)M_{22}^2 - \sin 2(\alpha - \beta)M_{12}^2, \quad (10)$$

$$\tan 2(\alpha - \beta) = \frac{2M_{12}^2}{M_{11}^2 - M_{22}^2}. \quad (11)$$

where the matrix elements are

$$\begin{aligned} M_{11}^2 &= v^2(\lambda_1 \cos^4 \beta + \lambda_2 \sin^4 \beta) + \frac{v^2}{2}(\lambda_3 + \lambda_4 + \lambda_5) \sin^2 2\beta, \\ M_{22}^2 &= M^2 + v^2 \sin^2 \beta \cos^2 \beta [\lambda_1 + \lambda_2 - 2(\lambda_3 + \lambda_4 + \lambda_5)], \\ M_{12}^2 &= \frac{v^2}{2} \sin 2\beta(-\lambda_1 \cos^2 \beta + \lambda_2 \sin^2 \beta) + \frac{v^2}{2} \sin 2\beta \cos 2\beta(\lambda_3 + \lambda_4 + \lambda_5). \end{aligned} \quad (12)$$

One of the most important variables in the active sector of the I(1+2)HDM, or equivalently in a 2HDM, is $\sin(\beta - \alpha)$. This describes deviations in the SM-like Higgs boson h couplings to gauge bosons and fermions. Namely, the ratios of the hVV ($V = W^\pm, Z$) and hff couplings in the I(1+2)HDM to those in the SM are given by

$$\frac{g_{hVV}^{\text{I(1+2)HDM}}}{g_{hVV}^{\text{SM}}} = \sin(\beta - \alpha), \quad \frac{g_{hff}^{\text{I(1+2)HDM}}}{g_{hff}^{\text{SM}}} = \sin(\beta - \alpha) + \xi_f \cos(\beta - \alpha), \quad (13)$$

where the ξ_f factors are $\cot \beta$ or $-\tan \beta$ depending on the type of fermion (i.e., up-type and down-type quarks and charged leptons) and the type of Yukawa interactions (i.e., the aforementioned 2HDM Types)⁴. The point here is that when we take the limit of $\sin(\beta - \alpha) \rightarrow 1$, both the hVV and hff couplings become the same as those in the SM. We thus call this limit the SM-like configuration. Furthermore, by looking at Eq. (12), we can see that only M_{22}^2 contains the term proportional to M^2 , while M_{11}^2 and M_{12}^2 are proportional to v^2 . Thus, when we take the limit of $M^2 \rightarrow \infty$, the mixing angle given in Eq. (11) becomes $\tan 2(\alpha - \beta) \rightarrow 0$, which also gives $m_H^2 \rightarrow M_{22}^2$ and $m_h^2 \rightarrow M_{11}^2$ by choosing $\alpha - \beta \rightarrow -\pi/2$. Therefore, the extra Higgs bosons H^\pm, A and H are decoupled due to the M^2 term in their mass formulae, so that we can call this limit the decoupling limit [31].

From the above discussion, we can reach an important conclusion regarding the nature of the Higgs sector in this model. The SM-like limit is naturally achieved when the decoupling limit is taken. In other words, the decoupling limit cannot be realized when we consider the case of a deviation from the SM-like limit, because we need a strong cancellation between M_{11}^2 and M_{22}^2 in the denominator of Eq. (11), in order to have $\tan 2(\alpha - \beta) \neq 0$. This would force the dimensionless coupling constants λ_i in the Higgs potential to acquire quite large values which must be excluded from the view point of ensuring perturbativity of the model. This in turn implies that there is an upper limit on the masses of the extra Higgs bosons when we consider the case of $\sin(\beta - \alpha) \neq 1$. As mentioned previously, one of the aims of this paper is indeed deriving an upper limit for these in the I(1+2)HDM by using bounds from vacuum stability and perturbative unitarity, which we will discuss in the next section.

⁴ The ξ_f factor corresponds to $2T_3^f \xi_A^f$ with T_3^f being the third component of the isospin, where ξ_A^f is given in Table II of Ref. [27].

C. Mass formulae in the I(2+1)HDM

Next, we present the mass formulae in the I(2+1)HDM. In this model, φ_0 corresponds to the SM Higgs doublet, so that H_0^\pm and A_0 correspond to the NG bosons G^\pm and G^0 , respectively, while H_0 is the SM-like Higgs boson h .

The mass of h is given just like the SM Higgs boson as

$$m_h^2 = 2\lambda_0 v^2. \quad (14)$$

In contrast, the inert sector is composed of two doublets, so that the masses for singly-charged, CP-odd and CP-even states are, respectively, given in the 2×2 matrix form. The mass matrix for the singly-charged scalar states is evaluated in the basis of (H_1^\pm, H_2^\pm) as

$$\mathcal{M}_C^2 = \begin{pmatrix} \mu_1^2 + \frac{v^2}{2}\rho_1 & \mu_{12}^2 \\ \mu_{12}^2 & \mu_2^2 + \frac{v^2}{2}\sigma_1 \end{pmatrix}, \quad (15)$$

and that for the CP-odd and CP-even states are given in the basis of (H_1, H_2) and (A_1, A_2) , respectively,

$$\mathcal{M}_A^2 = \mathcal{M}_C^2 + \frac{v^2}{2} \begin{pmatrix} \rho_2 - \rho_3 & 0 \\ 0 & \sigma_2 - \sigma_3 \end{pmatrix}, \quad \mathcal{M}_H^2 = \mathcal{M}_C^2 + \frac{v^2}{2} \begin{pmatrix} \rho_2 + \rho_3 & 0 \\ 0 & \sigma_2 + \sigma_3 \end{pmatrix}. \quad (16)$$

The mass eigenstates can be defined by introducing three mixing angles, as follows:

$$\begin{pmatrix} H_1^\pm \\ H_2^\pm \end{pmatrix} = R(\theta_C) \begin{pmatrix} \eta_1^\pm \\ \eta_2^\pm \end{pmatrix}, \quad \begin{pmatrix} A_1 \\ A_2 \end{pmatrix} = R(\theta_A) \begin{pmatrix} \eta_{A_1} \\ \eta_{A_2} \end{pmatrix}, \quad \begin{pmatrix} H_1 \\ H_2 \end{pmatrix} = R(\theta_H) \begin{pmatrix} \eta_{H_1} \\ \eta_{H_2} \end{pmatrix}. \quad (17)$$

The squared mass eigenvalues for the singly-charged states (η_1^\pm, η_2^\pm) are expressed in terms of the elements of the mass matrix as

$$m_{\eta_1^\pm}^2 = \cos^2 \theta_C (\mathcal{M}_C^2)_{11} + \sin^2 \theta_C (\mathcal{M}_C^2)_{22} + \sin 2\theta_C (\mathcal{M}_C^2)_{12}, \quad (18)$$

$$m_{\eta_2^\pm}^2 = \sin^2 \theta_C (\mathcal{M}_C^2)_{11} + \cos^2 \theta_C (\mathcal{M}_C^2)_{22} - \sin 2\theta_C (\mathcal{M}_C^2)_{12}, \quad (19)$$

while those for the CP-odd and CP-even states (η_{A_1}, η_{A_2}) and (η_{H_1}, η_{H_2}) , respectively, are obtained by replacing $(\theta_C, \mathcal{M}_C^2)$ with $(\theta_A, \mathcal{M}_A^2)$ and $(\theta_H, \mathcal{M}_H^2)$. Thus, the three mixing angles are given by

$$\tan 2\theta_X = \frac{2(\mathcal{M}_X^2)_{12}}{(\mathcal{M}_X^2)_{11} - (\mathcal{M}_X^2)_{22}}, \quad \text{for } X = C, A, H. \quad (20)$$

In summary, the inert sector of the I(2+1)HDM can be described by nine parameters: i.e., six masses $m_{\eta_i^\pm}$, $m_{\eta_{A_i}}$ and $m_{\eta_{H_i}}$ for $i = 1, 2$ and three mixing angles θ_X (for $X = C, A, H$). These nine physical parameters are expressed in terms of the nine parameters in the potential of Eq. (1): i.e., $\mu_1^2, \mu_2^2, \mu_{12}^2, \rho_i$ and σ_i ($i = 1, 2, 3$).

III. CONSTRAINTS ON THE PARAMETER SPACE

In this section, we discuss constraints on the parameter space in the I(1+2)HDM and the I(2+1)HDM. As theoretical constraints, we discuss bounds from vacuum stability and perturbative unitarity. As experimental constraints, other than ensuring sampling the 3HDM parameter spaces concerned away from experimental limits extracted via direct Higgs searches at LEP, Tevatron and LHC we also crucially take into account the so-called S , T and U parameters proposed by Peskin and Takeuchi [32] in the high precision EW fits to LEP data [33].

For the discussion of vacuum stability and unitarity, there is no difference between in the I(1+2)HDM and I(2+1)HDM. In contrast, for the S , T and U parameters, different formulae are presented here in each of two models.

A. Vacuum stability

The Higgs potential should be bounded from below in any direction of the scalar boson space. The sufficient condition to guarantee such a positivity of the potential is given by the following requirements:

$$\lambda_0 > 0, \quad \lambda_1 > 0, \quad \lambda_2 > 0, \tag{21}$$

$$\sqrt{\lambda_1 \lambda_2} + \lambda_3 + \text{MIN}(0, \lambda_4 + \lambda_5, \lambda_4 - \lambda_5) > 0, \tag{22}$$

$$\sqrt{\lambda_0 \lambda_1} + \rho_1 + \text{MIN}(0, \rho_2 + \rho_3, \rho_2 - \rho_3) > 0, \tag{23}$$

$$\sqrt{\lambda_0 \lambda_2} + \sigma_1 + \text{MIN}(0, \sigma_2 + \sigma_3, \sigma_2 - \sigma_3) > 0. \tag{24}$$

B. Unitarity

Constraints on the scalar self-coupling constants in the potential are extracted from the requirement of S -matrix unitarity for all the elastic scatterings of two body scalar boson states. This idea to constrain a scalar self-coupling has been proposed in Ref. [34] for the Higgs sector in the SM and it has been applied to constrain the mass of the SM Higgs boson. It can however be generalized to multi-doublet models, as well known [35]. The requirement of the S -matrix unitarity is translated into a relationship for the J th partial wave amplitude a_J . In the high energy limit, it can be expressed as

$$\text{Im}(a_J) = |a_J|^2. \tag{25}$$

This implies that a_J should be on a circle with radius and center of $1/2$ and $(0, 1/2)$ in the complex plane, respectively. From the above relation, we can require the following condition for the tree level amplitude of a_J as [35]

$$|\text{Re}(a_J)| < \frac{1}{2}. \quad (26)$$

In the high energy limit, each element of a_J for all possible $S_1 S_2 \rightarrow S_3 S_4$ processes, where the S_i 's represent all (pseudo)scalar bosons in the model, is simply given by the (pseudo)scalar four point interaction. In that case, only the s -wave amplitude ($J = 0$) can contribute to the scattering process. We thus apply the inequality given in Eq. (26) to the case of $J = 0$.

There are 30, 36 ($= 18 \times 2$) and 12 ($= 6 \times 2$) channels for electromagnetically neutral, singly-charged and doubly-charged states, respectively, where half of the singly- and doubly-charged states correspond to the charge conjugated states of the remaining half. Each channel classified by the difference in the Electro-Magnetic (EM) charge is orthogonal to the others, so that we can separately consider each of the channels. In order to distinguish these classes, we define a_0^N , a_0^C and a_0^D as the s -wave amplitude for the neutral, singly-charged and doubly-charged states, respectively.

In addition to the classification in terms of the EM charge, it is also helpful to distinguish the states by using the $Z_2 \times \tilde{Z}_2$ quantum numbers of the intervening external states. Because we are now focusing on the (pseudo)scalar boson quartic interactions only, the softly-broken \tilde{Z}_2 parity can be considered as the exact quantum number. Under $Z_2 \times \tilde{Z}_2$, four types of (pseudo)scalar pairings are allowed: i.e., $(Z_2, \tilde{Z}_2) = (+, +)$, $(+, -)$, $(-, +)$ and $(-, -)$, where each state does not mix with any other one. We thus further decompose the matrices for the s -wave amplitude into four sub-matrices as follows:

$$a_0^N = \text{diag} (a_{++}^N, a_{+-}^N, a_{-+}^N, a_{--}^N), \quad (27)$$

$$a_0^C = \text{diag} (a_{++}^C, a_{+-}^C, a_{-+}^C, a_{--}^C), \quad (28)$$

$$a_0^D = \text{diag} (a_{++}^D, a_{+-}^D, a_{-+}^D, a_{--}^D). \quad (29)$$

For the singly- and doubly-charged states, we focus on the 18[6] channels with the positive charge, because the remained negative charged states are connected by the charge conjugation as explained.

1. Neutral channels

We first consider the neutral channels. There are 12 pairings, $H_i^+ H_i^-$, $A_i A_i / \sqrt{2}$, $H_i H_i / \sqrt{2}$ and $A_i H_i$ ($i = 0, 1, 2$) with $(Z_2, \tilde{Z}_2) = (+, +)$. The 6 states with $(+, -)$ are $H_1^+ H_2^-$, $H_1^- H_2^+$,

A_1A_2 , H_1H_2 , A_1H_2 and H_1A_2 . The other states with $(-, +)$ and $(-, -)$ are respectively given by replacing the subscript of the $(+, -)$ states by $X_1Y_2 \rightarrow X_0Y_1$ and $X_1Y_2 \rightarrow X_0Y_2$. In fact, each sub-matrix in a_0^N can be made even simpler by choosing the following basis for the $(+, +)$ states:

$$|\Psi_{++}^N\rangle_{i+1} = \frac{1}{\sqrt{2}} \left(H_i^+ H_i^- + \frac{1}{\sqrt{2}} A_i A_i + \frac{1}{\sqrt{2}} H_i H_i \right), \quad (30)$$

$$|\Psi_{++}^N\rangle_{i+4} = \frac{1}{\sqrt{2}} \left(H_i^+ H_i^- - \frac{1}{\sqrt{2}} A_i A_i - \frac{1}{\sqrt{2}} H_i H_i \right), \quad (31)$$

$$|\Psi_{++}^N\rangle_{i+7} = \frac{1}{\sqrt{2}} (A_i A_i - H_i H_i), \quad (32)$$

$$|\Psi_{++}^N\rangle_{i+10} = A_i H_i, \quad \text{with } (i = 0, \dots, 2). \quad (33)$$

For the $(+, -)$ states, we can choose

$$|\Psi_{+-}^N\rangle_1 = \frac{1}{2} (H_1^+ H_2^- + H_1^- H_2^+ + A_1 A_2 + H_1 H_2), \quad (34)$$

$$|\Psi_{+-}^N\rangle_2 = \frac{1}{2} (-H_1^+ H_2^- - H_1^- H_2^+ + A_1 A_2 + H_1 H_2), \quad (35)$$

$$|\Psi_{+-}^N\rangle_3 = \frac{1}{2} (iH_1^+ H_2^- - iH_1^- H_2^+ - A_1 H_2 + H_1 A_2), \quad (36)$$

$$|\Psi_{+-}^N\rangle_4 = \frac{1}{2} (-iH_1^+ H_2^- + iH_1^- H_2^+ - A_1 H_2 + A_1 H_2), \quad (37)$$

$$|\Psi_{+-}^N\rangle_5 = \frac{i}{\sqrt{2}} (A_1 H_2 + H_1 A_2), \quad (38)$$

$$|\Psi_{+-}^N\rangle_6 = \frac{1}{\sqrt{2}} (-A_1 A_2 + H_1 H_2). \quad (39)$$

Similarly, the basis for the $(-, +)$ and $(-, -)$ states denoted as $|\Psi_{-+}^N\rangle_j$ and $|\Psi_{--}^N\rangle_j$ ($j = 1 \dots 6$) can be chosen by replacing the subscript in the above $(+, -)$ states by $X_1Y_2 \rightarrow X_0Y_1$ and $X_1Y_2 \rightarrow X_0Y_2$, respectively. In these basis, each sub-matrix in a_0^N can be block-diagonal form with a 3×3 sub-matrix as the largest one,

$$a_{++}^N = \frac{1}{16\pi} \text{diag} [(N_{++}^{3 \times 3})_1, (N_{++}^{3 \times 3})_2, (N_{++}^{3 \times 3})_3, (N_{++}^{3 \times 3})_4], \quad (40)$$

$$a_{+-}^N = \frac{1}{16\pi} \text{diag} [n_{+-}^1, n_{+-}^2, n_{+-}^3, n_{+-}^4, n_{+-}^5, n_{+-}^6], \quad (41)$$

$$a_{-+}^N = \frac{1}{16\pi} \text{diag} [n_{-+}^1, n_{-+}^2, n_{-+}^3, n_{-+}^4, n_{-+}^5, n_{-+}^6], \quad (42)$$

$$a_{--}^N = \frac{1}{16\pi} \text{diag} [n_{--}^1, n_{--}^2, n_{--}^3, n_{--}^4, n_{--}^5, n_{--}^6], \quad (43)$$

where

$$(N_{++}^{3 \times 3})_1 = \begin{pmatrix} 3\lambda_0 & 2\rho_1 + \rho_2 & 2\sigma_1 + \sigma_2 \\ 2\rho_1 + \rho_2 & 3\lambda_1 & 2\lambda_3 + \lambda_4 \\ 2\sigma_1 + \sigma_2 & 2\lambda_3 + \lambda_4 & 3\lambda_2 \end{pmatrix}, \quad (44)$$

$$(N_{++}^{3 \times 3})_2 = \begin{pmatrix} \lambda_0 & \rho_2 & \sigma_2 \\ \rho_2 & \lambda_1 & \lambda_4 \\ \sigma_2 & \lambda_4 & \lambda_2 \end{pmatrix}, \quad (45)$$

$$(N_{++}^{3 \times 3})_3 = (N_{++}^{3 \times 3})_4 = \begin{pmatrix} \lambda_0 & \rho_3 & \sigma_3 \\ \rho_3 & \lambda_1 & \lambda_5 \\ \sigma_3 & \lambda_5 & \lambda_2 \end{pmatrix}, \quad (46)$$

$$n_{+-}^1 = \lambda_3 + 2\lambda_4 + 3\lambda_5, \quad (47)$$

$$n_{+-}^2 = \lambda_3 + \lambda_5, \quad (48)$$

$$n_{+-}^3 = \lambda_3 - \lambda_5, \quad (49)$$

$$n_{+-}^4 = \lambda_3 + 2\lambda_4 - 3\lambda_5, \quad (50)$$

$$n_{+-}^5 = n_{+-}^6 = \lambda_3 + \lambda_4, \quad (51)$$

$$n_{-+}^1 = \rho_1 + 2\rho_2 + 3\rho_3, \quad (52)$$

$$n_{-+}^2 = \rho_1 + \rho_3, \quad (53)$$

$$n_{-+}^3 = \rho_1 - \rho_3, \quad (54)$$

$$n_{-+}^4 = \rho_1 + 2\rho_2 - 3\rho_3, \quad (55)$$

$$n_{-+}^5 = n_{-+}^6 = \rho_1 + \rho_2, \quad (56)$$

$$n_{--}^1 = \sigma_1 + 2\sigma_2 + 3\sigma_3, \quad (57)$$

$$n_{--}^2 = \sigma_1 + \sigma_3, \quad (58)$$

$$n_{--}^3 = \sigma_1 - \sigma_3, \quad (59)$$

$$n_{--}^4 = \sigma_1 + 2\sigma_2 - 3\sigma_3, \quad (60)$$

$$n_{--}^5 = n_{--}^6 = \sigma_1 + \sigma_2. \quad (61)$$

2. Singly-charged channels

Second, we consider the 18 positive singly-charged channels. The sub-matrix a_{++}^C has the form of 6×6 , while the sub-matrices a_{+-}^C , a_{-+}^C and a_{--}^C have the form of 4×4 . The basis

of a_{++}^C can be expressed as $(H_i^+ A_i, H_i^+ H_i)$ ($i = 0, \dots, 2$), and that of a_{+-}^C can be expressed by $(H_1^+ A_2, H_1^+ H_2, H_2^+ A_1, H_1^+ H_2)$. The basis for a_{-+}^C and a_{--}^C are respectively given by replacing the subscript of the basis for a_{+-}^C by $(1, 2) \rightarrow (0, 1)$ and $(1, 2) \rightarrow (0, 2)$.

By choosing the following basis, we obtain a further simplified form of each sub-matrix:

$$|\Psi_{++}^C\rangle_i = \frac{1}{\sqrt{2}} (iH_i^+ A_i + H_i^+ H_i), \quad (62)$$

$$|\Psi_{++}^C\rangle_{i+3} = \frac{1}{\sqrt{2}} (iH_i^+ A_i - H_i^+ H_i), \quad \text{with } (i = 0, \dots, 2), \quad (63)$$

$$|\Psi_{+-}^C\rangle_1 = \frac{1}{2} (iH_1^+ A_2 + H_1^+ H_2 + iA_1 H_2^+ + A_1 H_2^+), \quad (64)$$

$$|\Psi_{+-}^C\rangle_2 = \frac{1}{2} (iH_1^+ A_2 + H_1^+ H_2 - iA_1 H_2^+ - A_1 H_2^+), \quad (65)$$

$$|\Psi_{+-}^C\rangle_3 = \frac{1}{2} (iH_1^+ A_2 - H_1^+ H_2 + iA_1 H_2^+ - A_1 H_2^+), \quad (66)$$

$$|\Psi_{+-}^C\rangle_4 = \frac{1}{2} (iH_1^+ A_2 - H_1^+ H_2 - iA_1 H_2^+ + A_1 H_2^+). \quad (67)$$

The basis for the $(-, +)$ and $(-, -)$ states denoted as $|\Psi_{-+}^C\rangle_k$ and $|\Psi_{--}^C\rangle_k$ ($k = 1, \dots, 4$) can be chosen by replacing the subscript in the above $(+, -)$ states by $X_1 Y_2 \rightarrow X_0 Y_1$ and $X_1 Y_2 \rightarrow X_0 Y_2$, respectively. In this basis, each sub-matrix in a_0^C can be block-diagonal form as

$$a_{++}^C = \frac{1}{16\pi} \text{diag} [(C_{++}^{3 \times 3})_1, (C_{++}^{3 \times 3})_2], \quad (68)$$

$$a_{+-}^C = \frac{1}{16\pi} \text{diag} [c_{+-}^1, c_{+-}^2, c_{+-}^3, c_{+-}^4], \quad (69)$$

$$a_{-+}^C = \frac{1}{16\pi} \text{diag} [c_{-+}^1, c_{-+}^2, c_{-+}^3, c_{-+}^4], \quad (70)$$

$$a_{--}^C = \frac{1}{16\pi} \text{diag} [c_{--}^1, c_{--}^2, c_{--}^3, c_{--}^4], \quad (71)$$

where

$$(C_{++}^{3 \times 3})_1 = (N_{++}^{3 \times 3})_2, \quad (C_{++}^{3 \times 3})_2 = (N_{++}^{3 \times 3})_3, \quad (72)$$

$$c_{+-}^1 = n_{+-}^2, \quad (73)$$

$$c_{+-}^2 = n_{+-}^3, \quad (74)$$

$$c_{+-}^3 = n_{+-}^5, \quad (75)$$

$$c_{+-}^4 = \lambda_3 - \lambda_4, \quad (76)$$

$$c_{-+}^1 = n_{-+}^2, \quad (77)$$

$$c_{-+}^2 = n_{-+}^3, \quad (78)$$

$$c_{-+}^3 = n_{-+}^5, \quad (79)$$

$$c_{-+}^4 = \rho_1 - \rho_2, \quad (80)$$

$$c_{--}^1 = n_{--}^2, \quad (81)$$

$$c_{--}^2 = n_{--}^3, \quad (82)$$

$$c_{--}^3 = n_{--}^5, \quad (83)$$

$$c_{--}^4 = \sigma_1 - \sigma_2. \quad (84)$$

We note that c_{+-}^4 , c_{-+}^4 and c_{--}^4 give the independent eigenvalues against those in the neutral states.

3. Doubly-charged channels

Finally, we consider the 6 positive doubly-charged channels. The sub-matrix a_{++}^D has the form of 3×3 in the basis of $(H_i^+ H_i^+)/\sqrt{2}$ ($i = 0, \dots, 2$). Further, a_{+-}^D , a_{-+}^D and a_{--}^D have the 1×1 form for the $H_1^+ H_2^+$, $H_0^+ H_1^+$ and $H_0^+ H_2^+$ states, respectively. In the doubly-charged channels, the above basis gives already the simplest structure of the matrix of the s -wave amplitude, written as

$$a_{++}^D = \frac{1}{16\pi} (D_{++}^{3 \times 3}), \quad (85)$$

$$a_{+-}^D = \frac{1}{16\pi} d_{+-}, \quad (86)$$

$$a_{-+}^D = \frac{1}{16\pi} d_{-+}, \quad (87)$$

$$a_{--}^D = \frac{1}{16\pi} d_{--}. \quad (88)$$

They result in a 3×3 matrix with eigenvalues given as

$$(D_{++}^{3 \times 3}) = (N_{++}^{3 \times 3})_3, \quad (89)$$

$$d_{+-} = n_{+-}^5, \quad d_{-+} = n_{-+}^5, \quad d_{--} = n_{--}^5. \quad (90)$$

4. Summary

Consequently, we get 3 independent sub-matrices and 18 eigenvalues for a_0 . After we rename these, they are finally expressed by

$$X_1 = \begin{pmatrix} 3\lambda_0 & 2\rho_1 + \rho_2 & 2\sigma_1 + \sigma_2 \\ 2\rho_1 + \rho_2 & 3\lambda_1 & 2\lambda_3 + \lambda_4 \\ 2\sigma_1 + \sigma_2 & 2\lambda_3 + \lambda_4 & 3\lambda_2 \end{pmatrix}, \quad X_2 = \begin{pmatrix} \lambda_0 & \rho_2 & \sigma_2 \\ \rho_2 & \lambda_1 & \lambda_4 \\ \sigma_2 & \lambda_4 & \lambda_2 \end{pmatrix}, \quad X_3 = \begin{pmatrix} \lambda_0 & \rho_3 & \sigma_3 \\ \rho_3 & \lambda_1 & \lambda_5 \\ \sigma_3 & \lambda_5 & \lambda_2 \end{pmatrix}, \quad (91)$$

$$y_1^\pm = \lambda_3 + 2\lambda_4 \pm 3\lambda_5, \quad (92)$$

$$y_2^\pm = \rho_1 + 2\rho_2 \pm 3\rho_3, \quad (93)$$

$$y_3^\pm = \sigma_1 + 2\sigma_2 \pm 3\sigma_3, \quad (94)$$

$$y_4^\pm = \lambda_3 \pm \lambda_5, \quad (95)$$

$$y_5^\pm = \rho_1 \pm \rho_3, \quad (96)$$

$$y_6^\pm = \sigma_1 \pm \sigma_3, \quad (97)$$

$$y_7^\pm = \lambda_3 \pm \lambda_4, \quad (98)$$

$$y_8^\pm = \rho_1 \pm \rho_2, \quad (99)$$

$$y_9^\pm = \sigma_1 \pm \sigma_2. \quad (100)$$

The condition in Eq. (26) is expressed in terms of the above variables as

$$|x_i| < 8\pi, \quad (i = 1, \dots, 9), \quad (101)$$

$$|y_j^\pm| < 8\pi, \quad (j = 1, \dots, 9), \quad (102)$$

where x_i are the eigenvalues of X_1 , X_2 and X_3 .

We note that all the eigenvalues of the matrices given in Eq. (91) and those in Eqs. (92)-(100) coincide with those given in Ref. [20], in which the s wave amplitude matrix has been derived in the

S_3 symmetric version of the 3HDM, by taking the following replacement of the coupling constants

$$\begin{aligned}
\lambda_1 &\rightarrow 2(\lambda_1 + \lambda_3), & \lambda_2 &\rightarrow 2(\lambda_1 + \lambda_3), & \lambda_0 &\rightarrow 2\lambda_8, \\
\lambda_3 &\rightarrow 2(\lambda_1 - \lambda_3), & \lambda_4 &\rightarrow 2(-\lambda_2 + \lambda_3), & \lambda_5 &\rightarrow 2(\lambda_2 + \lambda_3), \\
\rho_1 &\rightarrow \lambda_5, & \rho_2 &\rightarrow \lambda_6, & \rho_3 &\rightarrow 2\lambda_7, \\
\sigma_1 &\rightarrow \lambda_5, & \sigma_2 &\rightarrow \lambda_6, & \sigma_3 &\rightarrow 2\lambda_7,
\end{aligned} \tag{103}$$

with taking λ_4 in Ref. [20] to be zero.

C. S , T and U parameters

We now discuss the S , T and U parameters in the context of our 3HDMs. The differences between the S , T and U parameters ($S_{3\text{HDM}}$, $T_{3\text{HDM}}$ and $U_{3\text{HDM}}$) and those in SM (S_{SM} , T_{SM} and U_{SM}), are defined by

$$\begin{aligned}
\Delta S &= S_{3\text{HDM}} - S_{\text{SM}}, \\
\Delta T &= T_{3\text{HDM}} - T_{\text{SM}}, \\
\Delta U &= U_{3\text{HDM}} - U_{\text{SM}}.
\end{aligned} \tag{104}$$

Throughout this subsection, we use the shortened notations $s_X \equiv \sin X$ and $c_X \equiv \cos X$.

In the I(1+2)HDM, the differences are composed of two parts: i.e., the contribution from active scalar boson loops and that from inert scalar boson loops. The former one is the same as in the 2HDM while the latter one is the same as in the IDM, which is composed of one active and one inert doublet fields. Therefore, ΔS , ΔT and ΔU can be just obtained by summing the two contributions, active (A) and inert (I), as

$$\begin{aligned}
\Delta S[\text{I}(1+2)\text{HDM}] &= \Delta S_A + \Delta S_I, \\
\Delta T[\text{I}(1+2)\text{HDM}] &= \Delta T_A + \Delta T_I, \\
\Delta U[\text{I}(1+2)\text{HDM}] &= \Delta U_A + \Delta U_I.
\end{aligned} \tag{105}$$

The S , T and U parameters in the 2HDM and IDM have been calculated in Ref. [36] and in Ref. [5],

respectively. Each of the differences is obtained as follows:

$$\begin{aligned} \Delta S_A &= \frac{1}{4\pi} \left\{ s_{\beta-\alpha}^2 F'(m_Z^2; m_H, m_A) - F'(m_Z^2; m_{H^\pm}, m_{H^\pm}) \right. \\ &\quad + c_{\beta-\alpha}^2 \left[F'(m_Z^2; m_h, m_A) + F'(m_Z^2; m_H, m_Z) - F'(m_Z^2; m_h, m_Z) \right] \\ &\quad \left. + 4m_Z^2 c_{\beta-\alpha}^2 \left[G'(m_Z^2; m_H, m_Z) - G'(m_Z^2; m_h, m_Z) \right] \right\}, \end{aligned} \quad (106)$$

$$\begin{aligned} \Delta T_A &= \frac{1}{16\pi^2 \alpha_{\text{em}} v^2} \left\{ F(0; m_{H^\pm}, m_A) + s_{\beta-\alpha}^2 [F(0; m_{H^\pm}, m_H) - F(0; m_A, m_H)] \right. \\ &\quad + c_{\beta-\alpha}^2 \left[F(0; m_{H^\pm}, m_h) + F(0; m_H, m_W) + F(0; m_h, m_Z) \right. \\ &\quad \left. - F(0; m_h, m_W) - F(0; m_A, m_h) - F(0; m_H, m_Z) \right] \\ &\quad \left. + 4G(0; m_H, m_W) + 4G(0; m_h, m_Z) - 4G(0; m_h, m_W) - 4G(0; m_H, m_Z) \right\}, \end{aligned} \quad (107)$$

$$\begin{aligned} \Delta U_A &= \frac{1}{4\pi} \left\{ F'(m_W^2; m_{H^\pm}, m_A) - F'(m_Z^2; m_{H^\pm}, m_{H^\pm}) \right. \\ &\quad + s_{\beta-\alpha}^2 [F'(m_W^2; m_{H^\pm}, m_H) - F'(m_Z^2; m_A, m_H)] \\ &\quad + c_{\beta-\alpha}^2 \left[F'(m_W^2; m_{H^\pm}, m_h) + F'(m_W^2; m_W, m_H) - F'(m_W^2; m_W, m_h) \right] \\ &\quad - c_{\beta-\alpha}^2 \left[F'(m_Z^2; m_A, m_h) + F'(m_Z^2; m_Z, m_H) - F'(m_Z^2; m_Z, m_h) \right] \\ &\quad + 4m_W^2 c_{\beta-\alpha}^2 \left[G'(m_W^2; m_H, m_W) - G'(m_W^2; m_h, m_W) \right] \\ &\quad \left. - 4m_Z^2 c_{\beta-\alpha}^2 \left[G'(m_Z^2; m_H, m_Z) - G'(m_Z^2; m_h, m_Z) \right] \right\}, \end{aligned} \quad (108)$$

$$\Delta S_I = \frac{1}{4\pi} \left[F'(m_Z^2; m_{\eta_H}, m_{\eta_A}) - F'(m_Z^2; m_{\eta^\pm}, m_{\eta^\pm}) \right], \quad (109)$$

$$\Delta T_I = \frac{1}{16\pi^2 \alpha_{\text{em}} v^2} \left[F(0; m_{\eta^\pm}, m_{\eta_A}) + F(0; m_{\eta^\pm}, m_{\eta_H}) - F(0; m_{\eta_A}, m_{\eta_H}) \right], \quad (110)$$

$$\begin{aligned} \Delta U_I &= \frac{1}{4\pi} \left[F'(m_W^2; m_{\eta^\pm}, m_{\eta_H}) + F'(m_W^2; m_{\eta^\pm}, m_{\eta_A}) \right. \\ &\quad \left. - F'(m_Z^2; m_{\eta^\pm}, m_{\eta^\pm}) - F'(m_Z^2; m_{\eta_H}, m_{\eta_A}) \right], \end{aligned} \quad (111)$$

where $F'(m_V^2; m_1, m_2) = [F(m_V^2; m_1, m_2) - F(0; m_1, m_2)]/m_V^2$ and $G'(m_V^2; m_1, m_2) =$

$[G(m_V^2; m_1, m_2) - G(0; m_1, m_2)]/m_V^2$. The loop functions are given by

$$F(p^2; m_1, m_2) = \int_0^1 dx \left[(2x-1)(m_1^2 - m_2^2) + (2x-1)^2 p^2 \right] \ln \Delta_B, \quad (112)$$

$$F(0; m_1, m_2) = \frac{1}{2}(m_1^2 + m_2^2) + \frac{2m_1^2 m_2^2}{m_1^2 - m_2^2} \ln \frac{m_2}{m_1}, \quad (113)$$

$$G(p^2; m_1, m_2) = \int_0^1 dx \ln \Delta_B, \quad (114)$$

$$G(0; m_1, m_2) = \ln(m_1 m_2) - \frac{m_1^2 + m_2^2}{m_1^2 - m_2^2} \ln \frac{m_2}{m_1} - 1, \quad (115)$$

$$\Delta_B = x m_1^2 + (1-x) m_2^2 - x(1-x) p^2. \quad (116)$$

We note that the functions F and G given in the above are invariant by interchanging the second and the third arguments; i.e., $F(p^2; m_1, m_2) = F(p^2; m_2, m_1)$ and $G(p^2; m_1, m_2) = G(p^2; m_2, m_1)$. We also note that ΔS_I , ΔT_I and ΔU_I are obtained by taking $\sin(\beta - \alpha) = 1$ and making the replacement $(m_{H^\pm}, m_A, m_H) \rightarrow (m_{\eta^\pm}, m_{\eta_A}, m_{\eta_H})$ in ΔS_A , ΔT_A and ΔU_A .

In the I(2+1)HDM, the differences purely come from the inert (pseudo)scalar boson loops. The

analytic expressions are given by

$$\Delta S = \frac{1}{4\pi} \left\{ -F'(m_Z^2; m_{\eta_1^\pm}, m_{\eta_1^\pm}) - F'(m_Z^2; m_{\eta_2^\pm}, m_{\eta_2^\pm}) \right. \\ \left. + c_{\theta_A - \theta_H} \left[F'(0; m_{\eta_{A_1}}, m_{\eta_{H_1}}) + F'(0; m_{\eta_{A_2}}, m_{\eta_{H_2}}) \right] \right. \\ \left. + s_{\theta_A - \theta_H} \left[F'(0; m_{\eta_{A_1}}, m_{\eta_{H_2}}) - F'(0; m_{\eta_{A_2}}, m_{\eta_{H_1}}) \right] \right\}, \quad (117)$$

$$\Delta T = \frac{1}{16\pi^2 \alpha_{\text{em}} v^2} \left\{ c_{\theta_C - \theta_A} \left[F(0; m_{\eta_1^\pm}, m_{\eta_{A_1}}) + F(0; m_{\eta_2^\pm}, m_{\eta_{A_2}}) \right] \right. \\ \left. + s_{\theta_C - \theta_A} \left[F(0; m_{\eta_1^\pm}, m_{\eta_{A_2}}) - F(0; m_{\eta_2^\pm}, m_{\eta_{A_1}}) \right] \right. \\ \left. + c_{\theta_C - \theta_H} \left[F(0; m_{\eta_1^\pm}, m_{\eta_{H_1}}) + F(0; m_{\eta_2^\pm}, m_{\eta_{H_2}}) \right] \right. \\ \left. + s_{\theta_C - \theta_H} \left[F(0; m_{\eta_1^\pm}, m_{\eta_{H_2}}) - F(0; m_{\eta_2^\pm}, m_{\eta_{H_1}}) \right] \right. \\ \left. - c_{\theta_A - \theta_H} \left[F(0; m_{\eta_{A_1}}, m_{\eta_{H_1}}) + F(0; m_{\eta_{A_2}}, m_{\eta_{H_2}}) \right] \right. \\ \left. - s_{\theta_A - \theta_H} \left[F(0; m_{\eta_{A_1}}, m_{\eta_{H_2}}) - F(0; m_{\eta_{A_2}}, m_{\eta_{H_1}}) \right] \right\}, \quad (118)$$

$$\Delta U = \frac{1}{4\pi} \left\{ -F'(m_Z^2; m_{\eta_1^\pm}, m_{\eta_1^\pm}) - F'(m_Z^2; m_{\eta_2^\pm}, m_{\eta_2^\pm}) \right. \\ \left. + c_{\theta_C - \theta_H} \left[F'(m_W^2; m_{\eta_1^\pm}, m_{\eta_{H_1}}) + F'(m_W^2; m_{\eta_2^\pm}, m_{\eta_{H_2}}) \right] \right. \\ \left. + s_{\theta_C - \theta_H} \left[F'(m_W^2; m_{\eta_1^\pm}, m_{\eta_{H_2}}) - F'(m_W^2; m_{\eta_2^\pm}, m_{\eta_{H_1}}) \right] \right. \\ \left. + c_{\theta_C - \theta_A} \left[F'(m_W^2; m_{\eta_1^\pm}, m_{\eta_{A_1}}) + F'(m_W^2; m_{\eta_2^\pm}, m_{\eta_{A_2}}) \right] \right. \\ \left. + s_{\theta_C - \theta_A} \left[F'(m_W^2; m_{\eta_1^\pm}, m_{\eta_{A_2}}) - F'(m_W^2; m_{\eta_2^\pm}, m_{\eta_{A_1}}) \right] \right. \\ \left. - c_{\theta_A - \theta_H} \left[F'(m_Z^2; m_{\eta_{A_1}}, m_{\eta_{H_1}}) + F'(m_Z^2; m_{\eta_{A_2}}, m_{\eta_{H_2}}) \right] \right. \\ \left. - s_{\theta_A - \theta_H} \left[F'(m_Z^2; m_{\eta_{A_1}}, m_{\eta_{A_2}}) - F'(m_Z^2; m_{\eta_{A_2}}, m_{\eta_{A_1}}) \right] \right\}. \quad (119)$$

The deviations in the S and T parameters from the SM predictions under $m_h = 126$ GeV and $U = 0$ are given by [33]

$$\Delta S = 0.05 \pm 0.09, \quad \Delta T = 0.08 \pm 0.07, \quad (120)$$

where the correlation factor between ΔS and ΔT is $+0.91$. We use the above experimental values for the numerical analysis in the next section.

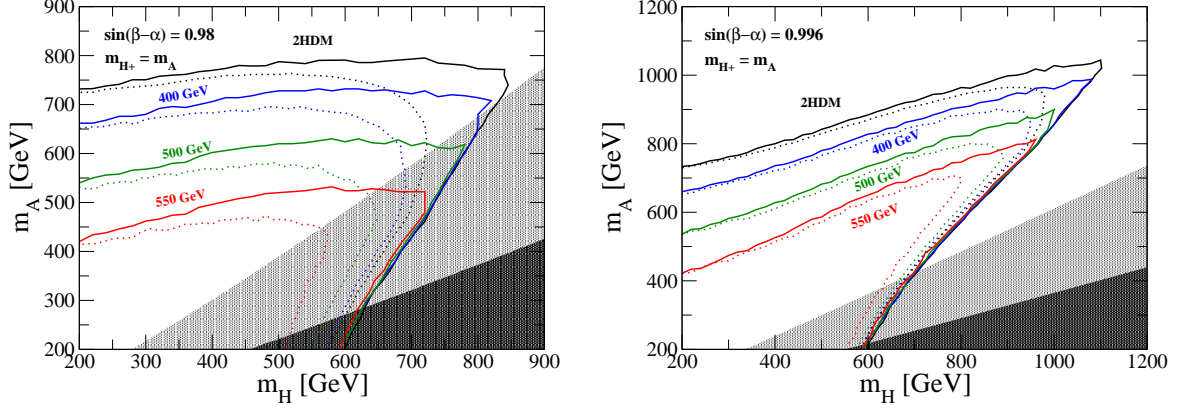


FIG. 1: Constraints on the I(1+2)HDM parameter space expressed in the the m_H - m_A plane induced by unitarity, vacuum stability and the S and T parameters in the case of $m_{H^\pm} = m_A$, $m_{\eta^\pm} = m_{\eta_H}$, $m_{\eta_A} = 63$ GeV and $\sin(\beta - \alpha) = 0.98$ (left panel) and 0.996 (right panel). We take $m_{\eta^\pm} = 400, 500$ and 550 GeV for the blue, green and red contours. We also show the result in the 2HDM as the black contour for comparison. The value of $\tan \beta$ is fixed to be 1 in the dotted contours while it is scanned over the range of $1 \leq \tan \beta \leq 30$ in the solid contours. For all the plots, we scan the value of M^2 in the range of $M^2 = m_H^2 \pm 1 \text{ TeV}^2$. The outside regions from each contour are excluded by unitarity and vacuum stability. The light and dark shaded regions are also excluded by S and T parameters in the 2HDM and I(1+2)HDM, respectively.

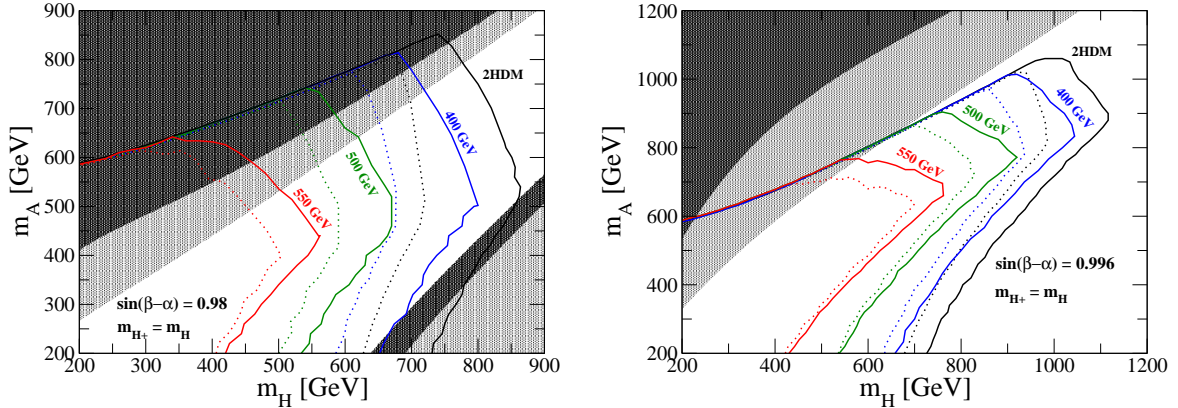


FIG. 2: Same as Fig. 1, but we take $m_{H^\pm} = m_H$ instead of $m_{H^\pm} = m_A$.

IV. NUMERICAL ANALYSIS

In this section, we discuss how the dimensionless quartic coupling constants in the scalar potential can be constrained from perturbative unitarity, vacuum stability and the S and T parameters in our 3HDMs. Among these coupling constants, λ_0 and $\lambda_{1,\dots,5}$ just describe four-point interactions

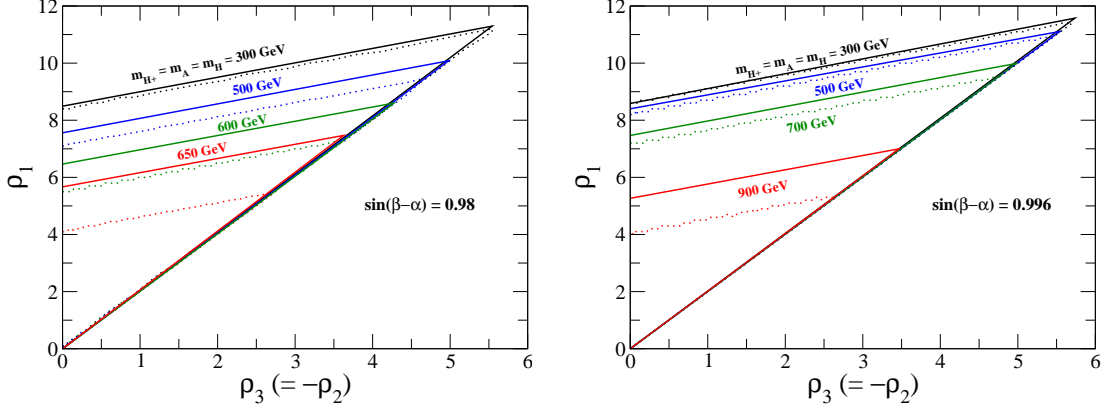


FIG. 3: Constraints on the I(1+2)HDM parameter space expressed in the ρ_3 - ρ_1 plane induced by unitarity and vacuum stability in the case of $m_{H^\pm} = m_A = m_H (\equiv m_\Phi)$, $m_{\eta^\pm} = m_{\eta_H}$, $m_{\eta_A} = 63$ GeV and $\sin(\beta - \alpha) = 0.98$ (left panel) and 0.996 (right panel). We take $m_\Phi = 300[300]$, $500[500]$, $600[700]$ and $650[900]$ GeV for the black, blue, green and red contours in the left[right] panel. The value of $\tan\beta$ is fixed to be 1 in the dotted contours, while it is scanned over the range of $1 \leq \tan\beta \leq 30$ in the solid contours. For all the plots, we scan the value of M^2 in the range of $M^2 = m_H^2 \pm 1 \text{ TeV}^2$. Outside regions from the contours are excluded by unitarity and vacuum stability.

among the inert (pseudo)scalar bosons in the I(1+2)HDM and I(2+1)HDM, respectively, and they do not affect to the active sector or the interaction between active and inert sectors at the tree level. We thus take these coupling constants to be zero in this section. We first show numerical results in the I(1+2)HDM and then in the I(2+1)HDM.

A. I(1+2)HDM

In the I(1+2)HDM, it is interesting to see how the constraints on the parameter space of the masses of active scalar bosons, H^\pm , A and H , can be modified by the requirement of unitarity and vacuum stability as compared to the 2HDM case. As we can see in the sections III-A and III-B, the additional coupling constants which do not enter in the 2HDM, such as ρ_i and σ_i , appear in the conditions of vacuum stability and unitarity. Therefore, a non-zero value of these coupling constants can modify the constraints on the parameters describing the active (2HDM-like) sector i.e., λ_1 - λ_5 , which are translated into bounds on the masses of active (pseudo)scalar bosons.

In the following, we fix the mass of either η_A or η_H to be $m_h/2 = 63$ GeV in order to satisfy the relic abundance of DM [37], and take all the other masses of the inert (pseudo)scalar bosons to be larger than $m_h/2$. For definiteness, we choose η_A as the DM candidate, so that we take

$m_{\eta_A} = m_h/2$. To avoid a large contribution to the T parameter, we take $m_{H^\pm} = m_A$ or $m_{H^\pm} = m_H$ and $m_{\eta^\pm} = m_{\eta_H}$. For simplicity, we take $\sigma_i = \rho_i$ ($i = 1, \dots, 3$). In that case, the coupling constants $\rho_{1, \dots, 3}$ are expressed in terms of the masses of inert scalar bosons as follows:

$$\rho_1 = \frac{2}{v^2}(m_{\eta^\pm}^2 - \mu_0^2), \quad (121)$$

$$\rho_2 = \frac{1}{v^2}(m_{\eta_H}^2 + m_{\eta_A}^2 - 2m_{\eta^\pm}^2) = \frac{1}{v^2}(m_{\eta_A}^2 - m_{\eta_H}^2), \quad (122)$$

$$\rho_3 = \frac{1}{v^2}(m_{\eta_H}^2 - m_{\eta_A}^2) = -\rho_2. \quad (123)$$

We can see that the sign of ρ_3 is now positive due to the assumption of $m_{\eta_A} = m_h/2$ ($< m_{\eta_H}$). The sign becomes negative when we consider the other case, of η_H as the DM candidate, but the bounds from vacuum stability and unitarity do not depend on the sign of ρ_3 . From the vacuum stability condition of (23), the value of ρ_1 should be larger than $2|\rho_2|$, thus we take $\rho_1 \gtrsim 2|\rho_2|$.

As we discussed in Sec. II-B, when $\sin(\beta - \alpha) \neq 1$ is taken, we cannot have the decoupling limit of the extra active Higgs bosons and thus we can obtain an upper limit of their masses. In addition, recall that the value of $\sin(\beta - \alpha)$ describes the deviation in the hVV couplings as shown in Eq. (13) at the tree level so that we may be able to find a relationship between the upper limit on the masses and the deviation in the hVV couplings. Because the $1\text{-}\sigma$ error of the measurement of hVV couplings is expected to be 2% at the HL-LHC and 0.4% at the ILC500 [11], we take $\sin(\beta - \alpha) = 0.98$ and 0.996 , respectively, as examples.

In Fig. 1, we show the constraint on the parameter space of the I(1+2)HDM mapped onto the m_H - m_A plane by unitarity, vacuum stability and the S and T parameters. We take $\sin(\beta - \alpha) = 0.98$ in the left panel and 0.996 in the right panel. The value of $\tan\beta$ is fixed to be 1 in the dotted contours, while it is scanned over the range $1 \leq \tan\beta \leq 30$ in the solid contours. For all the plots, we also scan the value of M^2 in the range of $M^2 = m_H^2 \pm 1 \text{ TeV}^2$. We check that these scanned ranges are enough wide to obtain the maximally allowed region on the parameter space from the unitarity and vacuum stability constraints. The blue, green and red contours show the cases of $m_{\eta^\pm} = 400, 500$ and 550 GeV, respectively. We also add a plot for the case in the 2HDM as the black contour for comparison. The regions outside each contour are excluded by unitarity and vacuum stability. In addition, the light and dark shaded regions are excluded by the S and T parameters in the 2HDM and I(1+2)HDM, respectively. We note that the contribution to ΔT is given to be zero due to $m_{H^\pm} = m_A$, so that the excluded region denoted by the light and dark area are from the constraint by ΔS . Besides, we confirm that the difference in ΔS due to the different choices of m_{η^\pm} is negligible.

In Fig. 2, we show the case of $m_{H^\pm} = m_H$ with the rest of the setup being the same as in Fig. 1.

In this case, there is a non-zero contribution to ΔT which is proportional to $\cos^2(\beta - \alpha)$, so that the excluded regions denoted by light and dark shading are different from those in Fig. 1.

We find that the upper limits on m_A and m_H are related to each other and are getting stronger by taking larger values of m_{η^\pm} . We note that, if we take the limit $m_{\eta^\pm}(= m_{\eta_H}) \rightarrow m_{\eta_A}$, the constraint from unitarity and vacuum stability approaches to that in the 2HDM.

In Fig. 3, we show the constraints on the parameter space on the ρ_3 - ρ_1 plane by unitarity and vacuum stability in the cases of $\sin(\beta - \alpha) = 0.98$ in the left panel and $\sin(\beta - \alpha) = 0.996$ in the right panel, where the regions outside each contour are excluded. The values of $\tan\beta$ and M^2 are taken as done in Figs. 1 and 2. The black, blue, green and red contours show the cases of $m_\Phi = 300[300, 500[500], 600[700]$ and $650[900]$ GeV in the left[right] panel, where $m_\Phi = m_{H^\pm} = m_A = m_H$. We note that the parameter space shown in this plot is allowed from the S and T parameters. We can see that the region with $\rho_1 < 2\rho_3$ is excluded by the vacuum stability condition in Eq. (23). Furthermore, the region above each contour is excluded by the unitarity constraints through the largest eigenvalue of the matrix X_1 given in Eq. (91).

B. I(2+1)HDM

Next, we consider an application of our bounds from unitarity and vacuum stability in the I(2+1)HDM. As mentioned in the beginning of this section, we take λ_1 - λ_5 to be zero. In that case, we obtain the analytic expression of the eigenvalues for three sub-matrices of the s -wave amplitude given in Eq. (91) as

$$O_1^T X_1 O_1 = \text{diag} \left(0, \frac{3\lambda_0}{2} \pm \sqrt{\frac{9}{4}\lambda_0^2 + (2\rho_1 + \rho_2)^2 + (2\sigma_1 + \sigma_2)^2} \right), \quad (124)$$

$$O_2^T X_2 O_2 = \text{diag} \left(0, \frac{\lambda_0}{2} \pm \sqrt{\frac{1}{4}\lambda_0^2 + \rho_2^2 + \sigma_2^2} \right), \quad (125)$$

$$O_3^T X_3 O_3 = \text{diag} \left(0, \frac{\lambda_0}{2} \pm \sqrt{\frac{1}{4}\lambda_0^2 + \rho_3^2 + \sigma_3^2} \right), \quad (126)$$

where $O_{1,\dots,3}$ are the orthogonal matrices to diagonalize $X_{1,\dots,3}$. Now, λ_0 is determined by $\lambda_0 = m_h^2/(2v^2) \simeq +0.13$ from Eq. (14), so that the positive eigenvalues are important to get a stronger bound.

In the following calculation, η_{A_1} is taken to be the DM candidate with mass $m_h/2$. For simplicity, we consider a no-mixing case between two inert scalar states, which can be realized by setting

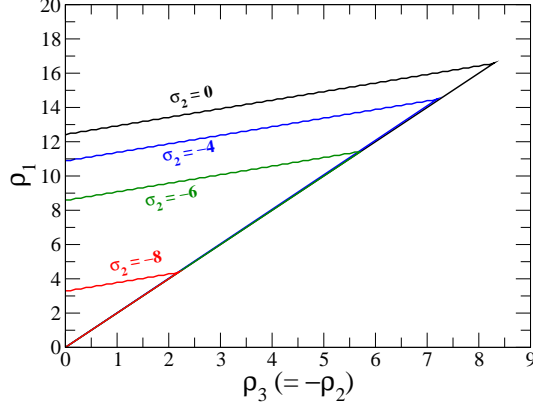


FIG. 4: Constraints on the I(2+1)HDM parameter space expressed in the ρ_3 - ρ_1 plane induced by unitarity and vacuum stability. Outside regions from the contours are excluded by unitarity and vacuum stability.

$\mu_{12}^2 \simeq 0^5$. In addition, to avoid the constraint from the T parameter, we take $m_{\eta_{H_1}} = m_{\eta_1^\pm}$ and $m_{\eta_{H_2}} = m_{\eta_2^\pm}$. We note that results do not change if we replace both[either] $m_{\eta_{H_1}}$ and[or] $m_{\eta_{H_2}}$ with $m_{\eta_{A_1}}$ and[or] $m_{\eta_{A_2}}$. In the above set up, we obtain the following relations for the quartic coupling constants:

$$\rho_2 = -|\rho_3|, \quad \sigma_2 = -|\sigma_3|. \quad (127)$$

From the vacuum stability condition in Eqs. (23) and (24), we have

$$\rho_1 > 2|\rho_2|, \quad \sigma_1 > 2|\sigma_2|. \quad (128)$$

By the combination of the bounds from unitarity and vacuum stability, the case with $\rho_1 \gtrsim 2|\rho_2|$ and $\sigma_1 \gtrsim 2|\sigma_2|$ gives the largest allowed parameter space. In this setup, we find that the eigenvalue of Eq. (124) gives the strongest bound.

In Fig. 4, we show the allowed parameter space mapped onto the ρ_3 - ρ_1 plane in the I(2+1)HDM. Regions outside the contours are excluded by unitarity and vacuum stability. More precisely, the region below the contour with $\rho_1 = 2\rho_3$ is excluded by vacuum stability and the region above the contour is excluded by unitarity.

⁵ When we take μ_{12}^2 to be exactly zero, the lightest state among η_{A_2} , η_{H_2} and η_2^\pm is also stable. In order to have a decay mode of it, a non-zero value of μ_{12}^2 is required.

V. CONCLUSIONS

We have discussed the constraints on the parameter space of the I(1+2)HDM and I(2+1)HDM emerging from the bounds on vacuum stability, perturbative unitarity and the EW S , T and U parameters. To impose the unitarity bound, we have calculated the s -wave amplitude matrix for all possible 2-to-2 body (pseudo)scalar boson elastic scatterings in the high energy limit by means of the ETA, where the sub-matrices with 30×30 , 36×36 and 12×12 forms for the electromagnetically neutral, singly-charged and doubly-charged channels, respectively, can be in block diagonal form with 3×3 sub-matrices as the largest component. We have first applied our formulae for the unitarity and vacuum stability bounds to constrain the parameter space in the I(1+2)HDM, especially mapped onto the m_H - m_A plane. We have found that larger excluded regions on such a plane can be obtained in the case with $\sin(\beta - \alpha) \neq 1$ as compared to those in 2HDMs. We then have applied our procedure to the I(2+1)HDM on the ρ_3 - ρ_1 plane. Here, it has been clarified that the values $\rho_3 \gtrsim 8, 7, 6$ and 2 are respectively excluded for any values of ρ_1 in the case of $\sigma_2 = 0, -4, -6$ and -8 .

Acknowledgments

S. M. is financed in part through the NExT Institute. Both authors acknowledge useful conversations with Venus Keus. K. Y. is supported by JSPS postdoctoral fellowships for research abroad.

-
- [1] [ATLAS Collaboration], Phys. Lett. B **716**, 1 (2012);
[CMS Collaboration], Phys. Lett. B **716**, 30 (2012).
 - [2] [ATLAS Collaboration], Report No. ATLAS-CONF-2013-034;
[CMS Collaboration], Report No. CMS-PAS-HIG-13-005.
 - [3] P. Fayet, Nucl. Phys. B **90**, 104 (1975).
 - [4] See, e.g., A. Zee, Phys. Lett. B **93**, 389 (1980) [Erratum-ibid. B **95**, 461 (1980)].
 - [5] R. Barbieri, L. J. Hall and V. S. Rychkov, Phys. Rev. D **74**, 015007 (2006).
 - [6] A. I. Bochkarev, S. V. Kuzmin and M. E. Shaposhnikov, Phys. Lett. B **244** (1990) 275;
A. E. Nelson, D. B. Kaplan and A. G. Cohen, Nucl. Phys. B **373**, 453 (1992);
N. Turok and J. Zadrozny, Nucl. Phys. B **369**, 729 (1992).
 - [7] H. Huffel and G. Pocsik, Z. Phys. C **8**, 13 (1981);
J. Maalampi, J. Sirkka and I. Vilja, Phys. Lett. B **265**, 371 (1991).
 - [8] S. Kanemura, T. Kubota and E. Takasugi, Phys. Lett. B **313**, 155 (1993);
A. G. Akeroyd, A. Arhrib and E. M. Naimi, Phys. Lett. B **490**, 119 (2000);

- I. F. Ginzburg and I. P. Ivanov, Phys. Rev. D **72**, 115010 (2005).
- [9] N. G. Deshpande and E. Ma, Phys. Rev. D **18**, 2574 (1978);
M. Sher, Phys. Rept. **179**, 273 (1989);
S. Nie and M. Sher, Phys. Lett. B **449**, 89 (1999);
S. Kanemura, T. Kasai and Y. Okada, Phys. Lett. B **471**, 182 (1999).
- [10] S. Kanemura, K. Tsumura, K. Yagyu and H. Yokoya, Phys. Rev. D **90**, 075001 (2014).
- [11] S. Dawson, A. Gritsan, H. Logan, J. Qian, C. Tully, R. Van Kooten *et al.*, arXiv:1310.8361 [hep-ex].
- [12] F. Gianotti, M. L. Mangano, T. Virdee *et al.*, Eur. Phys. J. C **39**, 293 (2005).
[ATLAS Collaboration], arXiv:1307.7292 [hep-ex];
[CMS Collaboration], arXiv:1307.7135.
- [13] See, e.g., R. G. Felipe, H. Serodio and J. P. Silva, Phys. Rev. D **87**, 055019 (2013).
- [14] F. Hartmann and W. Kilian, Eur. Phys. J. C **74**, 3055 (2014).
- [15] I. P. Ivanov and V. Keus, Phys. Rev. D **86**, 016004 (2012).
- [16] I. P. Ivanov and E. Vdovin, Eur. Phys. J. C **73**, 2309 (2013).
- [17] V. Keus, S. F. King and S. Moretti, JHEP **1401**, 052 (2014).
- [18] M. Maniatis and O. Nachtmann, arXiv:1408.6833 [hep-ph].
- [19] I. P. Ivanov and C. C. Nishi, JHEP **1501**, 021 (2015).
- [20] D. Das and U. K. Dey, Phys. Rev. D **89**, no. 9, 095025 (2014).
- [21] V. Keus, S. F. King and S. Moretti, Phys. Rev. D **90** (2014) 075015.
- [22] V. Keus, S. F. King, S. Moretti and D. Sokolowska, JHEP **1411**, 016 (2014).
- [23] A. G. Akeroyd, S. Moretti and J. Hernandez-Sanchez, Phys. Rev. D **85**, 115002 (2012) and arXiv:1409.7596 [hep-ph].
- [24] S. L. Glashow, S. Weinberg, Phys. Rev. D **15**, 1958 (1977).
- [25] V. D. Barger, J. L. Hewett and R. J. N. Phillips, Phys. Rev. D **41**, 3421 (1990);
Y. Grossman, Nucl. Phys. B **426**, 355 (1994).
- [26] A. G. Akeroyd, Phys. Lett. B **377**, 95 (1996).
- [27] M. Aoki, S. Kanemura, K. Tsumura and K. Yagyu, Phys. Rev. D **80**, 015017 (2009).
- [28] F. Mahmoudi and O. Stal, Phys. Rev. D **81**, 035016 (2010).
- [29] M. Aoki, R. Guedes, S. Kanemura, S. Moretti, R. Santos and K. Yagyu, Phys. Rev. D **84**, 055028 (2011).
- [30] C. W. Chiang and K. Yagyu, JHEP **1307**, 160 (2013).
- [31] J. F. Gunion and H. E. Haber, Phys. Rev. D **67**, 075019 (2003).
- [32] M. E. Peskin and T. Takeuchi, Phys. Rev. Lett. **65**, 964 (1990); Phys. Rev. D **46**, 381 (1992).
- [33] M. Baak, M. Goebel, J. Haller, A. Hoecker, D. Kennedy, R. Kogler, K. Moenig and M. Schott *et al.*, Eur. Phys. J. C **72**, 2205 (2012).
- [34] B. W. Lee, C. Quigg and H. B. Thacker, Phys. Rev. D **16**, 1519 (1977).
- [35] J. F. Gunion, H. E. Haber, G. L. Kane and S. Dawson, Front. Phys. **80**, 1 (2000).

- [36] D. Toussaint, Phys. Rev. D **18**, 1626 (1978);
S. Bertolini, Nucl. Phys. B **272**, 77 (1986);
W. Hollik, Z. Phys. C **32**, 291 (1986) and Z. Phys. C **37**, 569 (1988);
W. Grimus, L. Lavoura, O. M. Ogreid and P. Osland, Nucl. Phys. B **801**, 81 (2008) and Phys. Lett. B **704**, 303 (2011);
D. Lopez-Val and J. Sola, Eur. Phys. J. C **73**, 2393 (2013);
M. E. Peskin and J. D. Wells, Phys. Rev. D **64**, 093003 (2001);
S. Kanemura, Y. Okada, H. Taniguchi and K. Tsumura, Phys. Lett. B **704**, 303 (2011).
- [37] L. Lopez Honorez, E. Nezri, J. F. Oliver and M. H. G. Tytgat, JCAP **0702**, 028 (2007).
T. Hambye, F. -S. Ling, L. Lopez Honorez and J. Rocher, JHEP **0907**, 090 (2009) [Erratum-ibid. **1005**, 066 (2010)].